The glass half-empty: climate change drives lower freshwater input in the coastal system of the Chilean Northern Patagonia

Rodrigo Aguayo[1] · Jorge León-Muñoz[2,3] · José Vargas-Baecheler[1] · Aldo Montecinos[4,5] · René Garreaud[6,7] · Mauricio Urbina[8,9] · Doris Soto[3] · José Luis Iriarte[10,11]

Abstract

Oceanographic conditions in coastal Chilean northern Patagonia (41–46°S) are strongly influenced by freshwater inputs. Precipitation and streamflow records have shown a marked decrease in this area during the last decades. Given this hydro-climatic scenario, we evaluated the hydrological sensitivity driven by climate change in the Puelo River (average annual streamflow = 640 m^3 s^{-1}), one of the most important sources of freshwater in the fjords and inland seas of Chile's Northern Patagonia. A lumped hydrological model was developed to evaluate the potential impacts of climate change under the Representative Concentration Pathways (RCP) 2.6, 4.5, and 8.5 scenarios in the near future (2030–2060) using the delta change method based on 25 General Circulation Models. The model was fed by local hydro-meteorological data and remote sensors, simulating well the magnitude and seasonality of Puelo River streamflow. Considering the Refined Index of Agreement (RIA), the model achieved a high performance in the calibration (RIA = 0.79) and validation stages (RIA = 0.78). Under the RCP 8.5 scenario (multi-model mean), the projections suggest that the annual input of freshwater from the Puelo River to the Reloncaví Fjord would decrease by − 10% (1.6 km^3 less freshwater); these decreases would mainly take place in summer (~ − 20%) and autumn (~ − 15%). The recurrence of extreme hydroclimatic events is also projected to increase in the future, with the probability of occurrence of droughts, such as the recent 2016 event with the lowest freshwater input in the last 70 years, doubling with respect to the historical records.

✉ Jorge León-Muñoz
   jleon@ucsc.cl

Extended author information available on the last page of the article

🙋 Springer

1 Introduction

Signals of anthropogenic climate change are emerging rapidly both at global and local scales, including an overall increase in surface air temperature and changes in precipitation patterns. As a general rule, wet regions have seen an increase in precipitations, while subtropical regions became drier (Held and Soden 2006).

The influence of the Pacific Ocean and the Southern Hemisphere westerly wind belt produces high levels of precipitation (3000–4000 mm year^{-1}) at the Chilean Northern Patagonia coast (41–46°S), and further south inland the precipitation can exceed 7000 mm year^{-1}, due to the orographic effect of the Andes Range (Viale and Garreaud 2015). Moreover, the year-to-year precipitation variability is tightly coupled to the intensity of the westerly winds impinging the austral Andes (Garreaud et al. 2013). Since the 1970s, the Southern Annular Mode (SAM), an index that describes the movement of the low-pressure belt that generates westerly winds, has recorded a transition towards a positive phase, causing a decrease in the intensity of the westerly winds at midlatitudes (Garreaud et al. 2013). This shift of SAM towards its positive polarity has been attributed to stratospheric ozone reduction and increases in greenhouse gas concentration (Arblaster and Meehl 2006) and accounts for a significant fraction of the precipitation decrease in northern Patagonia (up to 7% per decade; Boisier et al. 2018) that has been evident for several decades (Garreaud et al. 2013; Boisier et al. 2018; León-Muñoz et al. 2018). Given this anomaly, streamflow of the main rivers has decreased noticeably during the dry seasons (Lara et al. 2008; Muñoz et al. 2016; León-Muñoz et al. 2018). The El Niño Southern Oscillation (ENSO) phenomenon also modulates the regional hydroclimate such that El Niño summers tends to produce dry conditions in northern Patagonia (e.g., Garreaud et al. 2009), with precipitation and streamflow lower than their historical averages (Garreaud 2018; León-Muñoz et al. 2018).

The marine coastal system of Chilean northern Patagonia is constituted by extensive and interconnected fjords, bays, and channels (~ 11,000 linear km of coastline), where the freshwater input (streamflow + precipitation) jointly with other factors like bathymetric, tidal, and wind patterns generate a strong estuarine circulation (Dávila et al. 2002). Specifically, freshwater input exerts a significant influence on the circulation patterns (i.e., rate of water renewal), biogeochemical processes (i.e., oxygenation and salinity), and energy transfer to different trophic levels (i.e., fisheries, mussel farming) (González et al. 2013; Torres et al. 2014; Castillo et al. 2016).

Reports of oceanographic anomalous events in Chilean northern Patagonia have been associated with the recent tendency of low freshwater input, especially in fjords, mainly during the El Niño (León-Muñoz et al. 2018). A weak haline stratification has been recorded in recent years on the Patagonian coast along with increased vertical mixing and advection of oceanic waters (León-Muñoz et al. 2013; Valle-Levinson et al. 2007). The weakly stratified water column in this fjord has been indicated to have two independent major implications: (1) during years of lower freshwater input it has been associated with ocean water masses with low dissolved oxygen levels (3 ml O_2 L^{-1}; León-Muñoz et al. 2013) and (2) enhancing periods of high phytoplankton biomass (Iriarte et al. 2017). Both of these are relevant for the fisheries and aquaculture developed in this region of Chile (Soto et al. 2019). One of the most extreme examples of these changes occurred during summer of 2016, when the joint effect of a strong El Niño event and a very positive SAM pattern resulted in a severe drought in southern Chile. As a result, the coastal surface layer received the lowest contribution of freshwater of the last

seven decades and was exposed to high radiation ranges (~ 30% higher on average). León-Muñoz et al. (2018) proposed that the decrease in freshwater input triggered the weakening of ocean stratification in the upper layer, thus allowing vertical advection of saline and nutrient-rich waters that, in conjunction with higher isolation, resulted in the enhanced harmful algal bloom (HAB). In fact, the HAB of *Pseudochattonella* cf. *verruculosa* produced losses of more than US$800 million in the salmon industry in just few days (Clément et al. 2016).

Climate projections for the coming decades indicate that the precipitation decrease should intensify in most of the Chilean territory (30–50°S; Boisier et al. 2016). The hydrological impacts of this trend have been mainly analyzed in the Mediterranean zone of Chile (30–37°S), where water demand is increasing (e.g., McPhee et al. 2010; Vicuña et al. 2012; Demaria et al. 2013; Bozkurt et al. 2018), while in the southern zone (> 41°S), where access to freshwater has not been a limiting factor in the past, it is becoming a concern for its consequences to aquaculture (Soto et al. 2019). Considering the observed impacts of drought upon coastal ecology—escalating in socio-economic disruptions—and that future freshwater input in western Patagonia is not clear, in this study we evaluated possible changes in surface hydrology in the austral Andes/western Patagonia driven by climate change. We particularly estimated the potential change in frequency of extreme hydrologic events such as that observed in early 2016. Specifically, we: (i) simulated the potential hydrological impacts on the Puelo River basin of the expected changes in temperature and precipitation for the RCP 2.6, RCP 4.5, and RCP 8.5 scenarios in the near future (2030–2060), and (ii) inferred foreseeable modifications in the regime and magnitude of the freshwater input to the inland sea of Chile's northern Patagonia. Puelo River is one of the most important sources of freshwater for the fjords and inland seas of Chile's northern Patagonia and an indicator of the behavior of many other rivers further south in this area (Lara et al. 2008). Given the complex topography and the mixed pluvio-nival hydrological regime of the rivers of this area, here we employed a lumped conceptual model fed with in situ and remote sensing data. We hypothesized that due to anthropogenic climate change, the freshwater input to the coastal system of Chilean northern Patagonia will have a different pattern in the near future, marked by a change in the annual hydrograph with a decrease in streamflow during spring (less snowmelt) and more intense and prolonged periods of dry season.

2 Methods

2.1 Study area

The hydrological model was implemented in the trans-Andean basin of the Puelo River (~ 9000 km², 66% Argentina, 34% Chile, Fig. 1), a well-preserved system where the landscape is dominated by native forest. The Puelo River has a strong influence on Reloncaví Fjord and Sound (41.5°S) (León-Muñoz et al. 2013), coastal areas which contribute approximately 12% of the Chilean salmon production, and more than 60% of mussel seeds that are farmed in Chile (Soto et al. 2019).

The streamflow and regime of the Puelo River adds the contributions of numerous tributaries, some of which include both Chilean and Argentinean territory (e.g., Manso River) and others that are only located in Chile (e.g., Ventisquero and Traidor Rivers) (Fig. 1).
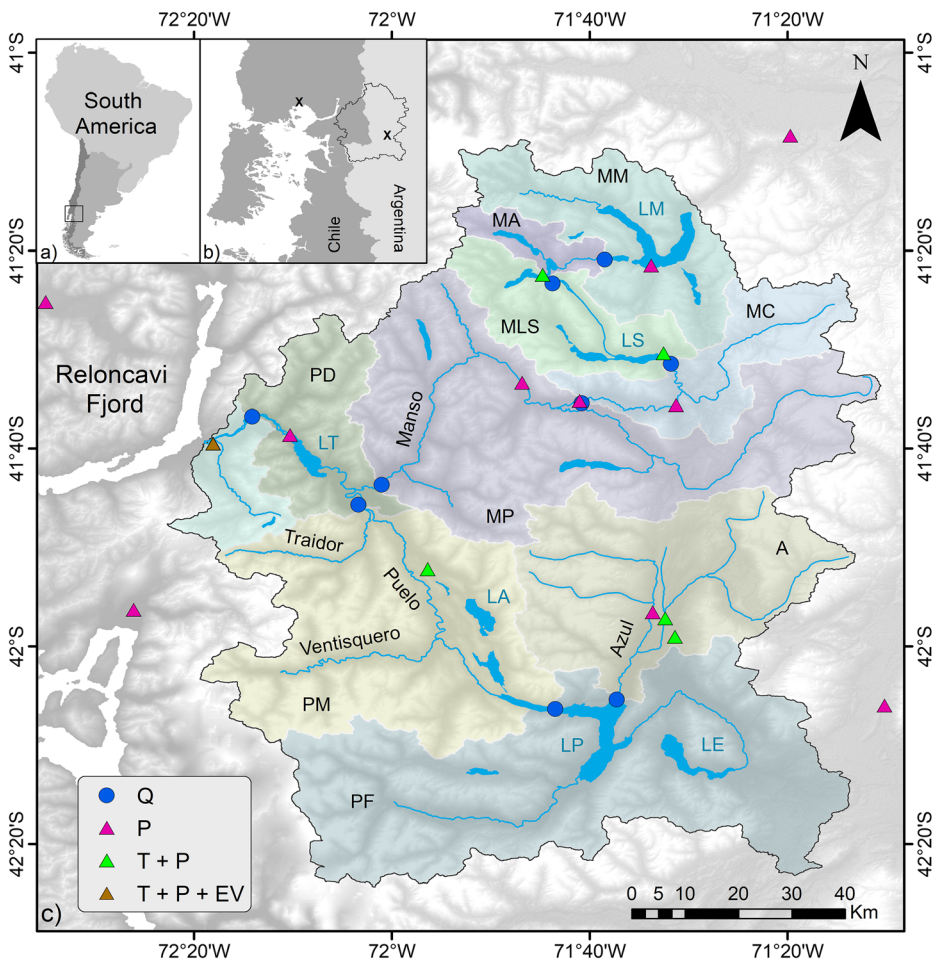
Fig. 1 **a** Puelo River Basin in relation to South America. **b** Puelo River Basin in the context of southern Chile/ Argentina. The letter X represents the precipitation stations of Puerto Montt city (Chile) and Puelo Lake (Argentina). **c** The Puelo River Basin and the Reloncaví Fjord. The monitoring stations used for the modeling are shown with blue circles for fluviometric stations (Q), purple triangles for rainfall stations (P), green triangles for those that measure temperature and rainfall (T+P), and brown triangle for the station that additionally measures evaporation (T+P+EV). The names identify the main rivers of the water network. The blue acronyms identify the main lakes (L) of the basin: LE = Epuyén, LP = Puelo, LA = Azul, LS = Steffen, LM = Mascardi, LT = Tagua-Tagua. The black acronyms indicate the names of the studied sub-basins (colored polygons): MM = Manso River in Moscos, MA = Manso River in Alerces, MLS = Manso River in Steffen Lake drainage, MC = Manso River in Confluence, MP = Manso River before Puelo, A = Azul River, PF = Puelo River in Puelo Lake drainage, PM = Puelo River before Manso River, PD = Puelo River before joining the Reloncaví Fjord

This basin contains more than 20 lakes in its water network, whose surface covers more than 200 km². Before flowing into the Reloncaví Fjord (41.4°S), the Puelo River has an average annual streamflow (Q) of 640 m³ s⁻¹, characterized by a pluvio-nival hydrological regime (850 m³ s⁻¹ in June and 760 m³ s⁻¹ in November; León-Muñoz et al. 2013) with a pattern similar to that described for the other main rivers of the northern zone of Chilean Patagonia (Petrohué Q = 320 m³ s⁻¹, Cochamó Q = 100 m³ s⁻¹, Yelcho Q = 360 m³ s⁻¹, Palena Q = 130 m³ s⁻¹, Cisnes Q = 240 m³ s⁻¹, Aysén Q = 630 m³ s⁻¹) (Lara et al. 2008).

2.2 Data

As with other Patagonian basins, the Puelo River has a low density of fluviometric and meteorological stations (Fig. 1). In fact, more than 75% of its drainage area is above the highest monitoring station (774 m.a.s.l.; Fig. S1). To address this lack of information, the input data used in the model was obtained by crossing information collected at local monitoring stations with the use of remote sensors. Thus, the data collected consisted of:

i) Bio-geographic characterization (CTS): the land cover was extracted from MCD12Q1 (Table S1; Friedl and Sulla-Menashe 2015) and the classification was based on the International Geosphere-Biosphere Program (IGBP; Hong and Adler 2008) (Fig. S2). The data was validated for both segments of the basin using vegetational cadastres produced by Chile and Argentina (INTA 2009; CONAF and UACh 2014). The soil hydrological classification was gathered from the Harmonized World Soil v1.2 database which contains the average granulometry of sand, silt and clay (Fig. S2).

ii) Hydro-meteorological data: local information on precipitation, temperature, streamflow, and lake level records were collected from the Water Resources Directorate of Chile and the Undersecretary of Water Resource of Argentina (Fig. 1). Additionally, radiosonde records collected in Puerto Montt were added (Fig. 1b) to obtain altitude data of the isotherm 0 °C. Only stations with more than 20 years of records and consistent data were selected, to that we applied a double-mass analysis to verify the consistency of the records. Information gaps (months with less than 10 days of records) were filled with linear regressions.

Precipitation (P): the location of the stations encouraged the use of remote sensors to capture the orographic gradients and increase the spatial representation of the Chilean section. Data were extracted from the remote sensor CHIRPSv2 (Table S1; Funk et al. 2015), which has shown good performance throughout Chile (Zambrano-Bigiarini et al. 2017). CHIRPSv2 was validated with local data and the biases found were corrected by the methodology proposed by Bhatti et al. (2016). The scheme consists of a scaling, where the ratio (BF) between the observed precipitation and that simulated by CHIRPSv2 was interpolated using ordinary kriging. Thus, for each month, the grid BF was multiplied by the grid given by CHIRPSv2 to obtain the final grilled fields.

Temperature (T): the limited number of stations and their low altitude motivated our use of product MODIS MOD11C3 (Table S1; Wan et al. 2015), which delivers surface temperature values. The biases were corrected by a multiple linear regression between the monthly day and night temperature, the elevation (explanatory variables), and the observed temperature. Other variables used in the literature such as vegetation indices (NVDI and EVI) were not statistically significant.

Snow cover area (SCA): we used the products MODIS MOD10A2 and MYD10A2 (Table S1; Hall et al. 2002) to calculate the basin area covered by snow. Our exploratory analysis of these information layers showed high cloud cover mainly in the winter months. To address this problem, the algorithm proposed by Dariane et al. (2017) was adapted, which uses the comparison of the two satellites, the elevation of each cell and a spatio-temporal filter (Text S1 and Fig. S3).

2.3 Hydrological modeling

We adapted a conceptual model for the Puelo River Basin with the approach used by Vargas et al. (2012) in the Simpson River Basin (~45°S), a model similar to the HBV model (Hydrologiska Byråns Vattenbalansavdelning). The river routing scheme consists of a lumped pattern across nine sub-basins (Figs. 1c and 2a), which were delimited considering the fluviometric stations (blue circles in Fig. 1). This approach was used considering that there is still no consensus regarding significant differences between the spatial representations (Vansteenkiste et al. 2014; and references therein). To improve the performance of this approach, we decided to get the input data (P, T, and SCA; monthly time step) by crossing information collected at local monitoring stations with that from remote sensors. Krogh et al. (2015) implemented the physical-based Cold Regions Hydrological Model (CRHM) in the Baker River Basin (~46°S) and concluded that the forced model with reanalysis data (ERA-Interim and CFSR) achieved better performance than the model based on scarce local data.

The main points of the hydrological model are the following (see Text S2 for more details):

– The snow routine uses a degree-day method, which calculates the snow reservoir (MM in Fig. 2b) and snowmelt, considering T and SCA of each sub-basin.
– The calculation for the surface runoff was made using the curve-number method based on the bio-geographic characterization (CTS in Fig. 2b; See Table S2 and Table S3).
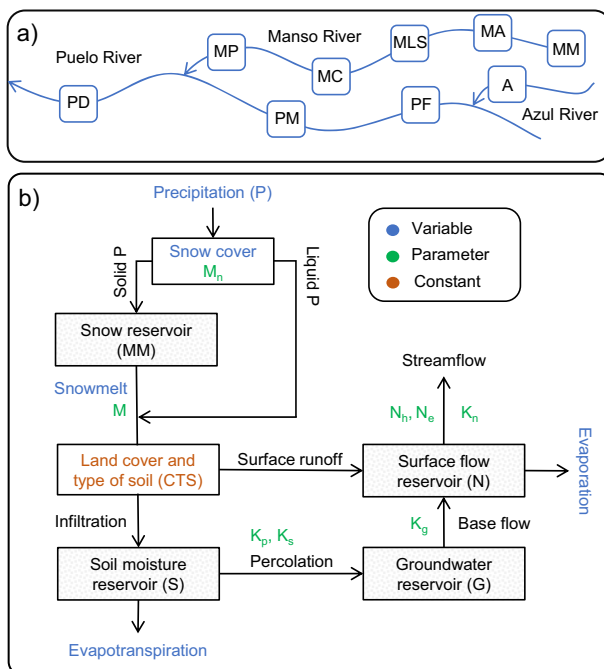
Fig. 2 Schematic hydrological model for the Puelo River Basin. **a** The lumped pattern across nine sub-basins; **b** The hydrological model for each sub-basin. The input variables of the model are indicated with blue letters; the constants in orange and the parameters in green. See Fig. 1 for the sub-basin acronyms and Table S4 for the description of the parameters

- The potential evapotranspiration (PET) was calculated using the Thornthwaite formula and the evaporation was estimated via an evaporimeter (located in the final section of Puelo River) as a function of PET ($R^2 = 0.89$, $p < 0.001$).
- In the presence of lakes, the simulated streamflow requires building "rating curves" between the lake water levels and their streamflow at the terminus of the sub-basins. The objective was to reproduce adequately the streamflow during the dry periods, which are not directly linked to precipitation patterns.

Model calibration involved adjusting the eight parameters based on the monthly streamflow in the nine sub-basins (Fig. 1). The calibration period spanned 2003–2010, while the validation was made for the 2010–2017 period. Our calibration strategy used a minimization of an objective function (Refined Index of Agreement, RIA; Willmott et al. 2012), which considered that the simulation of a drying climate requires a more balanced consideration of the mid-low streamflows and drier years in the calibration period as a closer analog of future conditions (Fowler et al. 2018). Calibration was performed for each sub-basin from upstream to downstream (Fig. 2), with the Excel Solver tool based on the nonlinear Generalized Reduced Gradient (GRG) resolution method with multiple-start (Arif et al. 2012), subject to the respective restrictions of each parameter (Table S4). In addition to RIA index, in the validation stage the Kling-Gupta Efficiency index (KGE; Kling et al. 2012) was added. The KGE index allowed evaluating the temporal dynamics (measured by linear correlation) and the preservation of the magnitude and variability of the streamflow.

2.4 Climate projections

Once the model was calibrated and validated, our objective was to evaluate the potential hydrological impacts that the predicted changes in air temperature and precipitation could have in the near future (2030–2060). We adopted the near future period (2030–2060) for two reasons. On one hand, a 20–40 year lead time minimizes the uncertainty of the climate projections (Hawkins and Sutton 2009). Shorter lead times (< 10 years) have large uncertainty dominated by internal variability (not fully resolved by the models) and the anthropogenic signal is still weak. Longer lead times (> 50 years) have large uncertainty inherited from the scenario ambiguity. On the other hand, we recognize that climate change is one among many stressors acting at the local level on the Patagonia water resources (e.g., damn constructions, aquaculture, forestry). It is too difficult to even anticipate the sign of those forcing in the far future, but one considers them stable in the next few decades, further supporting 2030–2060 as our target time period.

We applied the delta change approach (Diaz-Nieto and Wilby 2005) by the combination of precipitation (P) and air temperature (T) time series with General Circulation Model (GCM) simulations of the Coupled Model Intercomparison Project Phase 5 (CMIP5). Since a multimodel mean time series (temperature, precipitation, and other variables) robustly captures any possible trend arising from anthropogenic forcing, the year-to-year fluctuations are smoothed out in the average. For instance, many models do have a good representation of ENSO, but the occurrence of El Niño events (causing droughts in Patagonia) is completely asynchronous among those simulations, causing the multimodel mean series not to exhibit an El Niño year in the future. Therefore, we did not use the GCM climate projections directly, but instead we constructed plausible future climate scenarios for our target region by altering the original time series used for the

calibration and validation of the model (2003–2017, that does include ENSO events) with the climate-change signal (ΔP and ΔT).

A distinct set of precipitations and air temperatures (ΔP and ΔT) were defined for every month (i.e., 12 ΔP-ΔT pairs for each GCM) from the output of 42 runs from 25 GCMs for each scenario (RCP 2.6, RCP 4.5, and RCP 8.5), resulting in 126 plausible scenarios to occur in the near future. Specifically, the ranges of ΔP and ΔT for the near future were estimated for 2030–2060 using 1980–2010 as the base period. The delta approach renders our hydrological simulation independent of the GCM direct outputs, which certainly will include biases of different magnitude and sign in the current climate. We decided to employ all the models (each with its own set of delta factors) to enlarge the sample and provide a more robust estimate of the hydrological changes. The choice of employing the three emission scenarios was also grounded in the need to augment the sample of plausible futures.

In addition to the ΔP and ΔT pairs, we modified the snow cover area (SCA) used in the calibration and validation stages. For this, we assumed that the altitudinal temperature gradient (ΔT_h) will remain in the future, and the changes in temperature will modify the SCA according to the elevation of each sub-basin (Eq. 1),

$$\Delta SCA_i \ (\%) = \ \frac{\Delta T}{\Delta T_h \cdot (H_{max}{}^i - H_{min}{}^i)}, \tag{1}$$

where ΔSCA_i is the change of snow cover area and $H_{max}{}^i$ ($H_{min}{}^i$) is the maximum (minimum) elevation of sub-basin i. Finally, the future snow cover area was obtained by subtracting ΔSCA_i from the original series.

Similar to other regions of the world, inter-annual variability in the northern Patagonian zone is mainly produced by ENSO (Montecinos and Aceituno 2003; Garreaud et al. 2009). Global projections based on coupled ocean-atmosphere models still have no consensus regarding the future of ENSO variability (Collins et al. 2010), and the multi-model mean filters out most of the natural variability. Nevertheless, using the delta change approach preserves the observed (ENSO-related) variability, resulting in a reasonable modification of the climate conditions that includes natural variability and anthropogenic forcing.

3 Results

3.1 Hydro-climatic patterns

Using remote sensors and local hydro-meteorological data allowed us to understand the spatio-temporal patterns in the main input variables of the Puelo River Basin model. For precipitation, the results showed a clear differentiation between the western (3800 mm year^{-1}) and eastern (500 mm year^{-1}) sides of the Andes (Fig. 3a). This orographic effect is well known because during storm periods the forced ascent on the western slope of the Andes produces a marked increase in rainfall in that area, contrasting with the leeward rain shadow where the air descends (Smith and Evans 2007; Viale and Garreaud 2015). Thus, even though the area of the Puelo River Basin is mainly east of the Andes ($\sim$ 6000 km^2; 66%), the two sides of the Andes showed equal volumetric contributions of precipitation (50% each side). For temperature, the altitudinal temperature gradient was 5.3 °C km^{-1} (Fig. 3b). For snow cover (Fig. 3c), the Mann-Kendall test
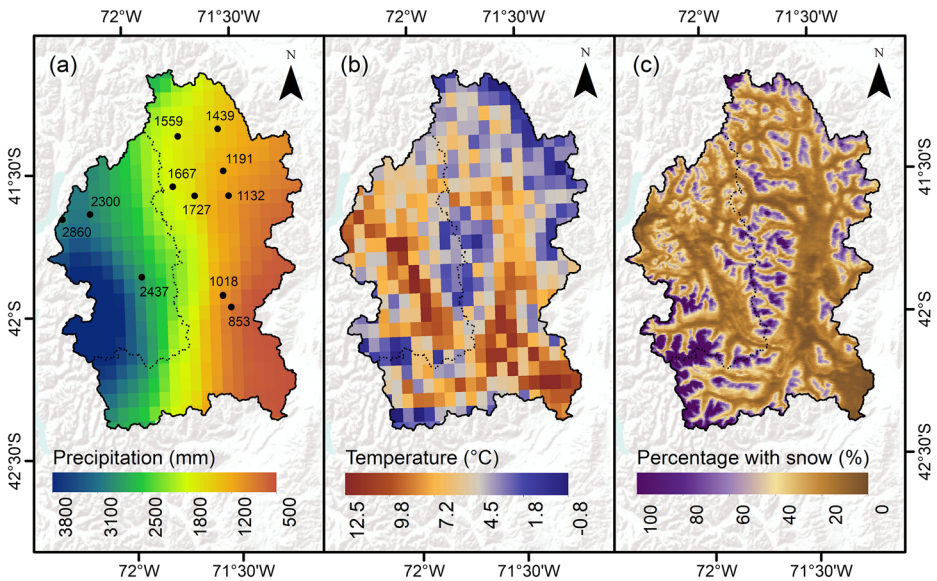
Fig. 3 Precipitation and temperature patterns and snow coverage of the Puelo River Basin for the period 2003–2017: **a** average annual rainfall from data processing of CHIRPSv2, the points indicate the local observations (see Fig. 1c), **b** average annual temperature from data processing of MOD11C3, **c** average annual snow cover area from data processing of MOD10A2, and MYD10A2 products

was applied to seasonal snow coverage area (SCA) and showed that summer (DJF) has a significant decrease ($p < 0.01$; Fig. 4a), similar to a temporal pattern found in other areas of Patagonia (46°S; Pérez et al. 2018). The Mann-Kendall test was also applied to the 0 °C isotherm to rule out the presence of inter-decade variability (limited temporal coverage of SCA). The results were consistent with SCA trend and showed an increase of 50 m per decade (Fig. 4b; $p < 0.05$).

According to the Standardized Streamflow Index (SSFI; Modarres 2007) and the Standardized Precipitation Index (SPI; Mckee et al. 1993), both calculated using 12 months as a time scale, precipitation and streamflow show a significant decrease in the Puelo basin (Fig. 4c). Specifically, the records of the Puelo River streamflow, a few kilometers before it drains into the Reloncaví Fjord (PD sub-basin) show a significant annual decrease (León-Muñoz et al. 2018), which is consistent with the pattern observed for the Manso River (sub-basins MA, MM, MLS and MC; Pasquini et al. 2008, 2013) and the overall drying trend in southern Chile (Boisier et al. 2018). According to the SSFI, the temporal pattern showed an increase in magnitude and duration of the drought periods since the beginning of the 1980s (Fig. 4c). These results were similar to those obtained from the SPI applied to the Puelo Lake precipitation records (Argentina) and the city of Puerto Montt (Chile) (see Fig. 1 for station locations). Both series also showed greater decoupling towards the current period, where drought scenarios generally tend to be more intense in the Chilean territory (e.g., period 2014–2018) (Fig. 4c). Additionally, we observed an amplification in the meteorological drought on the hydrological cycle in the years 1988/9, 1998/9, and 2015/6 (Fig. 4c). This process has been reported in central Chile, where the streamflow deficit can be twice as large as the precipitation deficit (Garreaud et al. 2017).
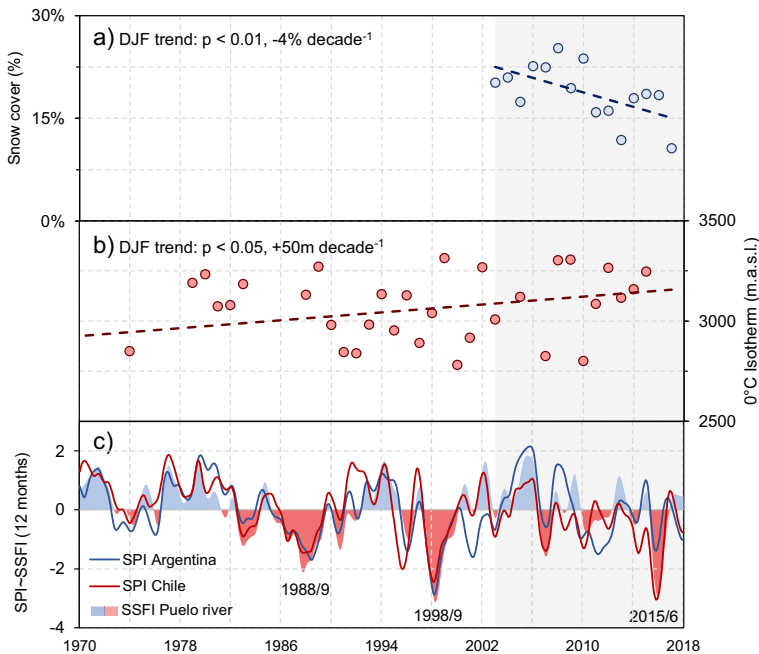
Fig. 4 **a** Standardized Streamflow Index (SSFI) of Puelo River and Standardized Precipitation Index (SPI) of Puelo Lake and the city of Puerto Montt (see Fig. 1b for station locations). **b** Trend analysis of snow cover (see Fig. 3c) for summer months from data processing of MOD10A2 and MYD10A2 products. **c** Trend analysis of the 0 °C isotherm obtained from the radiosonde of Puerto Montt. The gray zone indicates the period used for hydrological modeling

3.2 Hydrological modeling: present

The overall runoff processes and streamflow dynamics are well captured by the model. The calibration and validation stages of the hydrological model showed high values for the Kling-Gupta Efficiency index (KGE = 0.83) and Refined Index of Agreement (RIA = 0.75) (Table S5). In the final section of Puelo River (PD sub-basin), the model reached an RIA index of 0.79 and 0.78 in the calibration and validation stage, respectively. Thus, our approximation managed to simulate adequately the magnitude and seasonality of these records, showing a high level of coherence with respect to the innate variability of the streamflow regimes and the occurrence of floods and drought seasons (Fig. 5). This strong performance was achieved even under extremely dry conditions like summer and autumn, 2016, when streamflow was so low that the gaging station located before the mouth of the Puelo River in the Reloncaví Fjord remained above water level. For this period, the model reproduced a prolonged period of drought with extremely low monthly streamflow values (March–July 176 m^3 s^{-1}) compared to the average of the historical records (March–July 641 m^3 s^{-1}; Fig. 5).

In the snowmelt season (November to January), the model did not manage to simulate all the non-linearity of the observed series, and ultimately underestimated the peak of streamflow, because the role of snowmelt was not entirely captured ($\sim$ 5–15% in six of nine sub-basins; Fig. 5 and Fig. S4). With respect to evapotranspiration, we evaluated the uncertainty related to the application of a dependent temperature model (Thornthwaite equation) with an evaporimeter (Fig. 1).
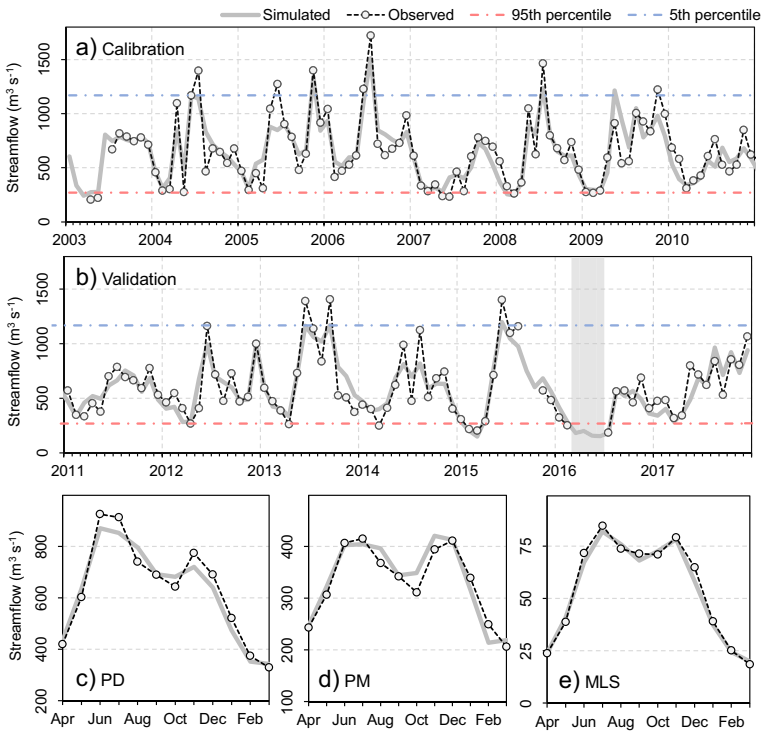
Fig. 5 Performance of the hydrological model during the **a** calibration and **b** validation stages for the final section of the Puelo River before emptying into the Reloncaví Fjord (PD sub-basin; Fig. 1). The gray column in (**b**) indicates where the gaging station did not report data (March–June of 2016). The lower boxes correspond show the performance of the hydrological model by monthly mean streamflow on **c** PD, **d** PM, and **e** MLS sub-basins (see Fig. 1)

The results indicate a good performance with a root-mean-square error of only 15 mm and the underestimation during the summers (DJF) is an order of magnitude smaller compared to the rainfall anomalies.

3.3 Climate projections

The results obtained from the GCM ensemble for the near future (2030–2060) in the Puelo River Basin showed high variability in temperature (ΔT) and precipitation (ΔPP) ranges in relation to the base period 1980–2010 (Fig. 6). The DFJ-MAM period will present higher seasonal rates of change (Fig. 6a–b), while for the JJA-SON period the changes are mostly attenuated and concentrated (Fig. 6c–d). Considering all seasons and RCPs scenarios, the results of the models (mean of RCPs) predict a marked annual decrease in precipitation (~10%) and increase in temperature (~1 °C). At the seasonal level, only 10% of the model outputs predict an increase in summer (DJF) precipitation, but such percentage increase to 30% in winter (JJA).

3.4 Hydrological modeling: near future

The streamflow series of the Puelo River (Figs. 1 and 2) was highly sensitive to the climate scenarios projected for the near future (2030–2060). Specifically, the decrease in precipitation
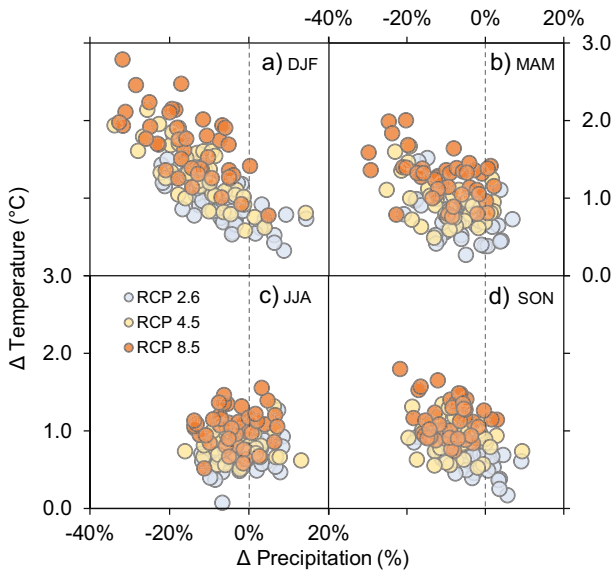
Fig. 6 Climate projections for each season (DJF, MAM, JJA, and SON) of precipitation and air temperature for the near future (period 2030–2060 vs. 1980–2010) according to data from 42 runs of 25 GCMs for each scenario (RCP 2.6, 4.5, and 8.5). The vertical line indicates $\Delta P = 0\%$

and the increase in air temperature cause an extension of the dry season and a transition to increasingly pluvial regimes, due to a decline in snow-covered area and an increase of rain-area contribution due to the direct effect of higher air temperatures (Fig. 7). Comparing the data modeled for the near future (multi-model average, RCP 8.5) to the present-day modeled streamflow, a strong decrease was predicted in the annual contributions of freshwater from the Puelo River to the Reloncaví Fjord (− 10%). These decreases would mainly take place in the summer (~ − 20%) and autumn (~ − 15%) months (Fig. 7). The smallest changes are projected for the winter months (Fig. 7).

Finally, we used the hydrological model to evaluate how bad the summer and autumn of 2016 was. The results indicated that there would be combinations of precipitation decrease and the increase of air temperature that could generate streamflow scenarios even lower than those observed during this period. The severity and frequency of extreme hydroclimatic events are also projected to increase in the future. In fact, the probability of occurrence of droughts, such as the recent 2016 event, doubles considering the historical records and the RCP 8.5 scenario (Fig. 8a–b). This ratio could even triple for the mid-low streamflow.

4 Discussion and conclusions

The evidence of large environmental change, such as interannual hydrological changes (decreasing pattern) in freshwater river inputs detected in northern Patagonia, may have several consequences for the basic functionalities and structure of coastal systems (fjords). In fact, comparing the historical records of streamflow with reconstructions made from dendrochronological studies, it is observed that the current trend exceeds in length, magnitude, and intensity what was estimated in previous centuries (Lara et al. 2008; Muñoz et al. 2016).
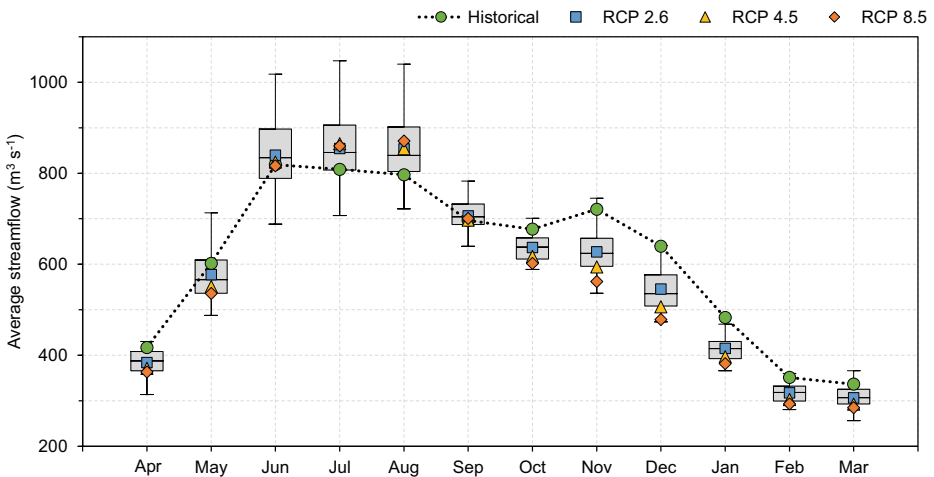
Fig. 7 Hydrological sensitivity of the Puelo River. The green circles indicate the monthly average streamflow of the period 2003–2017. The box plots represent the monthly streamflow modeled for the near future (2030–2060) according to the emission scenarios RCP 2.6, RCP 4.5, and RCP 8.5 (see Fig. 6)

The effect of this pattern, combined with regional climatic-oceanographic events (e.g., ENSO, SAM) and effects of local anthropogenic activities (e.g., nutrient fluxes from extensive aquaculture, land change due to forestry) may impact the chemical and physical properties of the surface water, destabilizing biological and chemical coastal processes (Iriarte 2018, Soto et al. 2019).

It is challenging to implement a hydrological model that can simulate adequately the hydrological behavior of the Puelo River, whose streamflow records are considered as a sentinel of the freshwater input in the semi-closed aquatic system of southern Chile (Lara et al. 2008; Iriarte et al. 2017). The hydro-meteorological information is scarce in Patagonia, especially in areas of low accessibility such as the trans-Andean basins of northern Patagonia, and therefore does not adequately represent the spatial-temporal gradients governing the hydrological processes. This low density of stations has been (in part) solved through the generation of input data from climatological reanalysis (e.g., Krogh et al. 2015). Given this situation, we concentrated efforts on strongly improving the scarce local data and choosing an appropriate objective function for a future drier climate. In doing so, we also recognized the high degree of uncertainty that is currently maintained for a large number of biogeographical and meteorological variables that support and validate more complex physically based models (e.g., relative humidity and wind speed for Penman-Monteith equation). Although the model performance obtained was adequate for the objectives of the study (KGE = 0.82 and RIA = 0.78 for the validation stage), the future implementation of more complex models needs to strengthen current monitoring systems (e.g., snow pillow and advanced meteorological stations) with the aim of validating and decreasing the gaps in understanding of the controlling variables in the hydrological cycle. This would allow the reduction of instances where the hydrological model over or underestimates streamflow, which tends to occur during the spring period, where the role of snowmelt was not entirely captured, given the uncertainties associated with the low-density gaging network, the parameter uncertainty and the model structure (Butts et al. 2004; Najafi et al. 2011; Poulin et al. 2011). It is also necessary to advance in the bio-geographic characterization of the main basins of southern Chile, with the aim of being
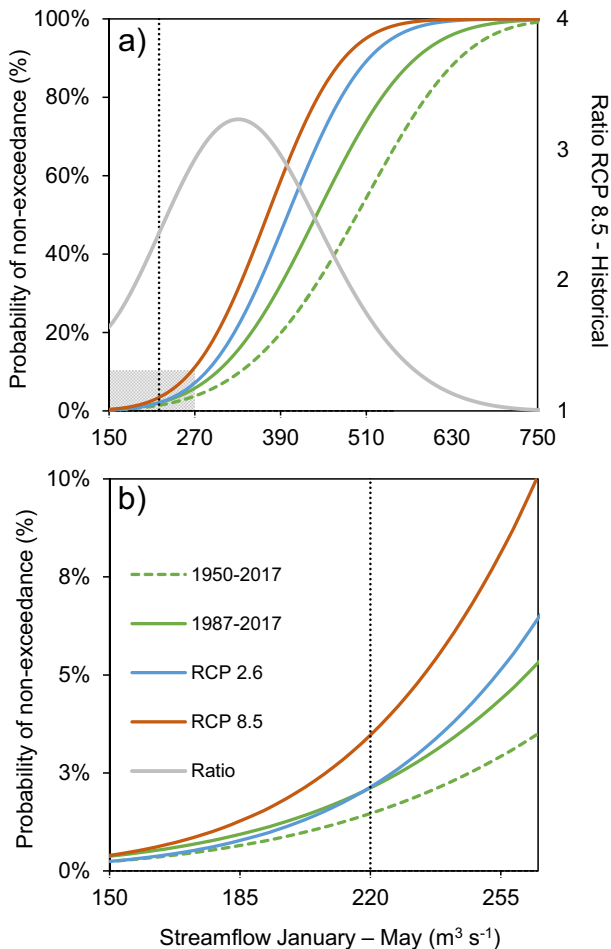
Fig. 8 a Comparison between accumulated distribution curves from the average streamflow for January–May: historical (1950–2017 and 1987–2017) and modeled under the scenarios RCP 2.6 and RCP 8.5. The continuous gray line indicate the ratio between the probability of the historical period (1950–2017) and the RCP 8.5 scenario. b The lower plot is an enlarged version of the gray box in Fig. 8a. The vertical discontinuous line indicates the modeled streamflow of 2016 when the station did not report data (Fig. 5)

able to implement properly more complex rainfall-runoff models and forecasting tools than those used in this study.

Although the variability is observed in the magnitude of the changes in climatic variables between different GCM models (e.g., Vicuña et al. 2012), the climate projections for the near future (2030–2060) are rather negative. Most GCM outputs indicate the continuation of the drying and warming trends, already evident since the 1970s (Boisier et al. 2018). The future trend is more evident—and uncertain—for the DFJ-MAM period ($\Delta PP = -10\% \pm 9\%$ and $\Delta T = +1.1 \pm 0.9\ °C$), where a decrease in precipitation is predicted by most model outputs, considering 1980–2010 as the baseline. We recognize that Patagonia's complex geography, including the austral Andes, multiple water bodies and its intricate coastline, renders a richly textured regional climate. Nonetheless, climate variability at seasonal and interannual time-scales is largely dictated by the strength of the Southern Hemisphere westerly winds (Garreaud

et al. 2013), a robust feature of the Earth's general circulation and adequately simulated by GCM (Yin 2005). Thus, while the GCM—by construction—do not capture the mesoscale details of the mean climate over Patagonia, they do have the Andes range and the impinging westerlies, the basic ingredients of the regional climate. It is also important to emphasize that the climate system shows long-term variability due to the Interdecadal Pacific Oscillation (IPO). The IPO is the result of the internal dynamics of the climate system and one of the main modes that affect the Pacific Ocean basin at this scale (Henley et al. 2015; and references therein). Therefore, the IPO can buffer or amplify the impacts associated with anthropogenic climate warming. However, according to the period of study for these areas of precipitation and temperature, no interdecadal variability was observed (Fig. S5).

Regardless of the chosen scenario, our results predict lower inputs of freshwater in the coastal system of northern Patagonia. While the model predicted a 10% decrease in annual mean streamflow for the next decades (mainly in the summer and autumn seasons), it also predicts a slight increase in streamflow during winter (+ 5%). This latter feature is puzzling, because in the near future the winter precipitation also decreases ($\Delta PP = -3 \pm 6\%$). In our model this is explained by the effect of the air temperature increase in the snow line (e.g., 1.0 °C = ~ 200 m higher in JJA). Given the complex terrain of northern Patagonia, this rise could translate into a larger area (e.g., 200 m = 10% more assuming the 0 °C isotherm at 1000 m.a.s.l.) receiving rain in the future (where currently snow falls) that is converted rapidly into surface runoff. Particular attention was placed on the occurrence of intense and extent droughts like that of 2016, the lowest freshwater input in the last seven decades. This event had dramatic impacts upon coastal ecosystems (León-Muñoz et al. 2018) and severely affected aquaculture activities such as salmon and mussel farming, affecting industries that directly or indirectly employ a high percentage of the population of these areas (Soto et al. 2019). Since the delta approach preserves the structure of natural variability and dry summer conditions are mostly associated with ENSO events (Garreaud 2018), we found that the frequency and intensity of such extremely dry conditions will be twice as likely to occur as in the present (Fig. 8; assuming that natural inter-annual variability will remain similar in the next decades).

Even recognizing the intrinsic uncertainties of the hydrological modeling process, which are considerably less than the uncertainty of the climate projections (Najafi et al. 2011), there is a very high probability that for the oncoming period of 2030–2060 climate change could further exacerbate the effects of low freshwater inputs on coastal systems, increasing their exposure to anomalous events with strong socio-economic repercussions/conflicts. It is compulsory to evaluate the consequences of the projected change at river basin scale in connection with the marine ecosystem. This is rarely done, but we believe is essential to prepare local plans to deal with climate change, making fisheries and aquaculture more resilient to future changes (Bueno and Soto 2017). The maintenance/intensification of interannual hydro-climatic trends (decrease in precipitation and in increase temperature and therefore streamflow) and the increase in extreme events (e.g., strong annual precipitation anomalies) make the coastal zone of northern Patagonia vulnerable to the effects of climate change (Soto et al. 2019).

These anomalous events are relevant considering that Chile is currently the second world producer and exporter of farmed salmon (~ 522,000 tons with a value of US$4.650 million in 2017) and the first exporter of farmed mussels (~ 80,000 tons with a value of US$210 million in 2017). Both salmon farming and mussel farming can be strongly influenced by freshwater inputs and associated changes in salinity and temperature. For example, to maintain certain local oceanographic circulation conditions that facilitate mussel larvae transport to be captured by mussel collectors, a key stage in mussel farming (Molinet et al. 2017). Additionally, one of

the most relevant health problems for salmon farming is the external parasite sea lice and it is well known that the parasite does not perform well below 25 of salinity (Montory et al. 2018). In fact, these parasite outbreaks are far lower in areas with higher freshwater input. A similar situation is observed in the case of gill amebiasis which also affects farmed salmon in more saline waters (Soto et al. 2019). Nowadays, up to 35% of current Chilean salmon farming takes place in fjords in areas with strong to moderate freshwater influence (Soto et al. 2019). The effectiveness of several pharmaceuticals to treat sea lice also varies as function of salinity and temperature, and therefore changes in the coastal dynamics might have broad implication for the economic activities developing in the northern Patagonia (Urbina et al. 2019). Considering this, a better understanding of the driving factors forcing future changes (i.e., modifications in the outflow patterns) is essential for the adaptation of the aquaculture industry and local fisheries. Thus, we considered it relevant to consider our results to advance in actions that increase the resilience of the land-ocean interface to climate change, such as: (i) strengthen and expand the hydro-climatic (high zones of the basins) and oceanographic monitoring systems in Patagonia; (ii) construct and/or validate new hydrological models that could serve as early warning systems and estimate the risks of HAB occurrence and other changes in the marine ecosystem that may affect aquaculture, fishing, and other activities; and (iii) protect the high level of conservation that the landscape of northern Patagonian that still has. The basins of this region still maintain high native forest cover with practically no regulation and/or derivation of their waters (e.g., reservoirs, irrigation). These attributes will help to maximize and ensure good standards of water supply under less friendly climatic scenarios.

References

Arblaster J, Meehl G (2006) Contributions of external forcings to southern annular mode trends. J Clim 19:2896–2905. https://doi.org/10.1175/JCLI3774.1

Arif C, Setiawan BI, Mizoguchi M, Doi R (2012) Estimation of water balance components in Paddy fields under non-flooded irrigation regimes by using excel solver. J Agron 11:53–59. https://doi.org/10.3923/ja.2012.53.59

Bhatti HA, Rientjes T, Haile AT et al (2016) Evaluation of bias correction method for satellite-based rainfall data. Sensors (Switzerland) 16:1–16. https://doi.org/10.3390/s16060884

Boisier JP, Rondanelli R, Garreaud R, Muñoz F (2016) Anthropogenic and natural contributions to the Southeast Pacific precipitation decline and recent megadrought in Central Chile. Geophys Res Lett 43:413–421. https://doi.org/10.1002/2015GL067265

Boisier JP, Alvarez-Garreton C, Cordero RR, et al (2018) Anthropogenic drying in central-southern Chile evidenced by long-term observations and climate model simulations Elem Sci Anthr 6 doi: https://doi.org/10.1525/elementa.328/

Bozkurt D, Rojas M, Boisier JP, Valdivieso J (2018) Projected hydroclimate changes over Andean basins in Central Chile from downscaled CMIP5 models under the low and high emission scenarios. Clim Change 1–17. https://doi.org/10.1007/s10584-018-2246-7

Bueno P, Soto D (2017) Adaptation strategies of the aquaculture sector to the impacts of climate change. FAO Fisheries and Aquaculture Circular No. 1142. FAO, Rome

Butts MB, Payne JT, Kristensen M, Madsen H (2004) An evaluation of the impact of model structure on hydrological modelling uncertainty for streamflow simulation. J Hydrol 298:242–266. https://doi.org/10.1016/j.jhydrol.2004.03.042

Castillo MI, Cifuentes U, Pizarro O et al (2016) Seasonal hydrography and surface outflow in a fjord with a deep sill: the Reloncaví fjord, Chile. Ocean Sci 12:533–534. https://doi.org/10.5194/os-12-533-2016

Clément A, Lincoqueo L, Saldivia M et al (2016) Exceptional summer conditions and HABs of Pseudochattonella in southern Chile create record impacts on Salmon farms. HAN 53:1–3

Collins M, An S-I, Cai W et al (2010) The impact of global warming on the tropical Pacific Ocean and El Niño. Nat Geosci 3:391–397. https://doi.org/10.1038/ngeo868

CONAF, UACh (2014) Monitoreo de cambios, corrección cartográfica y actualización del catastro de recursos Vegetacionales Nativos de la Región de Los Lagos. Valdivia, Chile

Dariane AB, Khoramian A, Santi E (2017) Remote sensing of environment investigating spatiotemporal snow cover variability via cloud-free MODIS snow cover product in central Alborz region. Remote Sens Environ 202:152–165. https://doi.org/10.1016/j.rse.2017.05.042

Dávila PM, Figueroa D, Müller E (2002) Freshwater input into the coastal ocean and its relation with the salinity distribution off austral Chile (35–55°S). Cont Shelf Res 22:521–534. https://doi.org/10.1016/S0278-4343(01)00072-3

Demaria EMC, Maurer EP, Thrasher B et al (2013) Climate change impacts on an alpine watershed in Chile: do new model projections change the story? J Hydrol 502:128–138. https://doi.org/10.1016/j.jhydrol.2013.08.027

Diaz-Nieto J, Wilby RL (2005) A comparison of statistical downscaling and climate change factor methods: impacts on low flows in the river Thames, United Kingdom. Clim Chang 69:245–268. https://doi.org/10.1007/s10584-005-1157-6

Fowler K, Peel M, Western A, Zhang L (2018) Improved rainfall-runoff calibration for drying climate: choice of objective function. Water Resour Res 54:3392–3408. https://doi.org/10.1029/2017WR022466

Friedl M, Sulla-Menashe D (2015) MCD12Q1 MODIS/Terra+aqua land cover type yearly L3 global 500m SIN grid V006 [data set]. NASA EOSDIS Land Processes DAAC

Funk C, Peterson P, Landsfeld M et al (2015) The climate hazards infrared precipitation with stations - a new environmental record for monitoring extremes. Sci Data 2:1–21. https://doi.org/10.1038/sdata.2015.66

Garreaud R (2018) Record-breaking climate anomalies lead to severe drought and environmental disruption in western Patagonia in 2016. Clim Res 74:217–229. https://doi.org/10.3354/cr01505

Garreaud R, Vuille M, Compagnucci R, Marengo J (2009) Present-day south American climate. Palaeogeogr Palaeoclimatol Palaeoecol 281:180–195. https://doi.org/10.1016/j.palaeo.2007.10.032

Garreaud R, Lopez P, Minvielle M, Rojas M (2013) Large-scale control on the Patagonian climate. J Clim 26:215–230. https://doi.org/10.1175/JCLI-D-12-00001.1

Garreaud R, Alvarez-Garreton C, Barichivich J et al (2017) The 2010-2015 mega drought in Central Chile: impacts on regional hydroclimate and vegetation. Hydrol Earth Syst Sci 21:6307. https://doi.org/10.5194/hess-2017-191

González HE, Castro LR, Daneri G et al (2013) Land–ocean gradient in haline stratification and its effects on plankton dynamics and trophic carbon fluxes in Chilean Patagonian fjords (47–50°S). Prog Oceanogr 119:32–47. https://doi.org/10.1016/j.pocean.2013.06.003

Hall K, Riggs GA, Salomonson VV, Goddard N (2002) MODIS snow-cover products. Remote Sens Environ 83:181–194. https://doi.org/10.1016/S0034-4257(02)00095-0

Hawkins E, Sutton R (2009) The potential to narrow uncertainty in regional climate predictions. Bull Am Meteorol Soc 90:1095–1108. https://doi.org/10.1175/2009BAMS2607.1

Held IM, Soden BJ (2006) Robust responses of the hydrological cycle to global warming. J Clim 19:5686–5699. https://doi.org/10.1175/JCLI3990.1

Henley BJ, Gergis J, Karoly DJ et al (2015) A Tripole index for the Interdecadal Pacific oscillation. Clim Dyn 45:3077–3090. https://doi.org/10.1007/s00382-015-2525-1

Hong Y, Adler RF (2008) Estimation of global SCS curve numbers using satellite remote sensing and geospatial data. Int J Remote Sens 29:471–477. https://doi.org/10.1080/01431160701264292

INTA (2009) Monitoreo de la Cobertura y el Uso del Suelo a partir de sensores remotos. Argentina

Iriarte JL (2018) Natural and human influences on marine processes in Patagonian Subantarctic coastal waters. Front Mar Sci 5:360. https://doi.org/10.3389/fmars.2018.00360

Iriarte JL, León-Muñoz J, Marcé R et al (2017) Influence of seasonal freshwater streamflow regimes on phytoplankton blooms in a Patagonian fjord. New Zeal J Mar Freshw Res 51:304–315. https://doi.org/10.1080/00288330.2016.1220955

Kling H, Fuchs M, Paulin M (2012) Runoff conditions in the upper Danube basin under an ensemble of climate change scenarios. J Hydrol 424–425:264–277. https://doi.org/10.1016/j.jhydrol.2012.01.011

Krogh SA, Pomeroy JW, Mcphee J (2015) Physically based mountain hydrological modeling using reanalysis data in Patagonia. J Hydrometeorol 16:172–193. https://doi.org/10.1175/JHM-D-13-0178.1

Lara A, Villalba R, Urrutia R (2008) A 400-year tree-ring record of the Puelo River summer-fall streamflow in the Valdivian rainforest eco-region, Chile. Clim Chang 86:331–356. https://doi.org/10.1007/s10584-007-9287-7

León-Muñoz J, Marcé R, Iriarte JL (2013) Influence of hydrological regime of an Andean river on salinity, temperature and oxygen in a Patagonia fjord, Chile. New Zeal J Mar Freshw Res 47:515–528. https://doi.org/10.1080/00288330.2013.802700

León-Muñoz J, Urbina MA, Garreaud R, Iriarte JL (2018) Hydroclimatic conditions trigger record harmful algal bloom in western Patagonia (summer 2016). Sci Rep 8:1330. https://doi.org/10.1038/s41598-018-19461-4

Mckee TB, Doesken NJ, Kleist J (1993) The relationship of drought frequency and duration to time scales. Proc 8th Conf Appl Climatol 17:179–184

McPhee J, Rubio-Alvarez E, Meza R et al (2010) An approach to estimating hydropower impacts of climate change from a regional perspective. In: Watershed management 2010. American Society of Civil Engineers, Reston, pp 13–24

Modarres R (2007) Streamflow drought time series forecasting. Stoch Environ Res Risk Assess 21:223–233. https://doi.org/10.1007/s00477-006-0058-1

Molinet C, Díaz M, Marín SL et al (2017) Relation of mussel spatfall on natural and artificial substrates: analysis of ecological implications ensuring long-term success and sustainability for mussel farming. Aquaculture 467:211–218. https://doi.org/10.1016/j.aquaculture.2016.09.019

Montecinos A, Aceituno P (2003) Seasonality of the ENSO-related rainfall variability in Central Chile and associated circulation anomalies. J Clim 16:281–296. https://doi.org/10.1175/1520-0442(2003)016<0281:SOTERR>2.0.CO;2

Montory JA, Cumillaf JP, Cubillos VM et al (2018) Early development of the ectoparasite Caligus rogercresseyi under combined salinity and temperature gradients. Aquaculture 486:68–74. https://doi.org/10.1016/j.aquaculture.2017.12.017

Muñoz AA, González-Reyes A, Lara A et al (2016) Streamflow variability in the Chilean temperate-Mediterranean climate transition (35°S–42°S) during the last 400 years inferred from tree-ring records. Clim Dyn 47:4051–4066. https://doi.org/10.1007/s00382-016-3068-9

Najafi MR, Moradkhani H, Jung IW (2011) Assessing the uncertainties of hydrologic model selection in climate change impact studies. Hydrol Process 25:2814–2826. https://doi.org/10.1002/hyp.8043

Pasquini AI, Lecomte KL, Depetris PJ (2008) Climate change and recent water level variability in Patagonian proglacial lakes, Argentina. Glob Planet Change 63:290–298. https://doi.org/10.1016/j.gloplacha.2008.07.001

Pasquini AI, Lecomte KL, Depetris PJ (2013) The Manso glacier drainage system in the northern Patagonian Andes: an overview of its main hydrological characteristics. Hydrol Process 27:217–224. https://doi.org/10.1002/hyp.9219

Pérez T, Mattar C, Fuster R (2018) Decrease in snow cover over the Aysén river catchment in Patagonia, Chile. Water (Switzerland) 10:1–16. https://doi.org/10.3390/w10050619

Poulin A, Brissette F, Leconte R et al (2011) Uncertainty of hydrological modelling in climate change impact studies in a Canadian, snow-dominated river basin. J Hydrol 409:626–636. https://doi.org/10.1016/j.jhydrol.2011.08.057

Smith RB, Evans JP (2007) Orographic precipitation and water vapor fractionation over the southern Andes. J Hydrometeorol 8:3–19. https://doi.org/10.1175/JHM555.1

Soto D, León-Muñoz J, Dresdner J, et al (2019) Salmon farming vulnerability to climate change in southern Chile: understanding the biophysical, socioeconomic and governance links. Rev Aquac Raq 12336. https://doi.org/10.1111/raq.12336

Torres R, Silva N, Reid B, Frangopulos M (2014) Silicic acid enrichment of subantarctic surface water from continental inputs along the Patagonian archipelago interior sea (41–56°S). Prog Oceanogr 129:50–61. https://doi.org/10.1016/j.pocean.2014.09.008

Urbina MA, Cumillaf JP, Paschke K, Gebauer P (2019) Effects of pharmaceuticals used to treat salmon lice on non-target species: evidence from a systematic review. Sci Total Environ 649:1124–1136. https://doi.org/10.1016/j.scitotenv.2018.08.334

Valle-Levinson A, Sarkar N, Sanay R et al (2007) Spatial structure of hydrography and flow in a Chilean fjord, Estuario Reloncaví. Estuar Coasts 30:113–126. https://doi.org/10.1007/BF02782972

Vansteenkiste T, Tavakoli M, Van Steenbergen N et al (2014) Intercomparison of five lumped and distributed models for catchment runoff and extreme flow simulation. J Hydrol 511:335–349. https://doi.org/10.1016/j.jhydrol.2014.01.050

Vargas J, De La Fuente L, Arumí JL (2012) Balance hídrico mensual de una cuenca Patagónica de Chile: Aplicación de un modelo parsimonioso. Obras Proy 12:32–41. https://doi.org/10.4067/S0718-28132012000200003

Viale M, Garreaud R (2015) Orographic effects of the subtropical and extratropical Andes on upwind precipitating clouds. J Geophys Res Atmos 120:4962–4974. https://doi.org/10.1002/2014JD023014

Vicuña S, McPhee J, Garreaud R (2012) Agriculture vulnerability to climate change in a snowmelt-Driven Basin in semiarid Chile. J Water Resour Plan Manag 138:431–441. https://doi.org/10.1061/(ASCE)WR.1943-5452.0000202

Wan Z, Hook S, Hulley G (2015) MOD11C3 MODIS/Terra land surface temperature/emissivity monthly L3 global 0.05Deg CMG V006 [data set]

Willmott CJ, Robeson SM, Matsuura K (2012) A refined index of model performance. Int J Climatol 32:2088–2094. https://doi.org/10.1002/joc.2419

Yin JH (2005) A consistent poleward shift of the storm tracks in simulations of 21st century climate. Geophys Res Lett 32. https://doi.org/10.1029/2005GL023684

Zambrano-Bigiarini M, Nauditt A, Birkel C et al (2017) Temporal and spatial evaluation of satellite-based rainfall estimates across the complex topographical and climatic gradients of Chile. Hydrol Earth Syst Sci 21:1295–1320. https://doi.org/10.5194/hess-21-1295-2017

Publisher's note Springer Nature remains neutral with regard to jurisdictional claims in published maps and institutional affiliations.

Affiliations

Rodrigo Aguayo[1] · Jorge León-Muñoz[2,3] · José Vargas-Baecheler[1] · Aldo Montecinos[4,5] · René Garreaud[6,7] · Mauricio Urbina[8,9] · Doris Soto[3] · José Luis Iriarte[10,11]

[1] Departamento de Ingeniería Civil, Facultad de Ingeniería, Universidad de Concepción, Concepción, Chile

[2] Departamento de Química Ambiental, Facultad de Ciencias, Universidad Católica de la Santísima Concepción, Concepción, Chile

[3] Centro Interdisciplinario para la Investigación Acuícola (INCAR), Concepción, Chile

[4] Departamento de Geofísica, Facultad de Ciencias Físicas y Matemáticas, Universidad de Concepción, Concepción, Chile

[5] Centro de Recursos Hídricos para la Agricultura y Minería (CRHIAM), Concepción, Chile

[6] Departamento de Geofísica, Facultad de Ciencias Físicas y Matemáticas, Universidad de Chile, Santiago, Chile

[7] Centro de Ciencia del Clima y la Resiliencia (CR^2), Santiago, Chile

[8] Departamento de Zoología, Facultad de Ciencias Naturales y Oceanográficas, Universidad de Concepción, Concepción, Chile

[9] Instituto Milenio de Oceanografía (IMO), Universidad de Concepción, Concepción, Chile

[10] Instituto de Acuicultura, Centro de Investigación Dinámica de Ecosistemas Marinos de Altas Latitudes (IDEAL), Universidad Austral de Chile, Puerto Montt, Chile

[11] Centro de Investigación Oceanográfica COPAS Sur-Austral, Universidad de Concepción, Concepción, Chile